



AMS
American Meteorological Society

Supplemental Material

Journal of Climate

Recent Trends in Summer Atmospheric Circulation in the North Atlantic/European Region: Is
There a Role for Anthropogenic Aerosols?
<https://doi.org/10.1175/JCLI-D-20-0665.1>

© [Copyright 2021 American Meteorological Society](#) (AMS)

For permission to reuse any portion of this work, please contact permissions@ametsoc.org. Any use of material in this work that is determined to be “fair use” under Section 107 of the U.S. Copyright Act (17 USC §107) or that satisfies the conditions specified in Section 108 of the U.S. Copyright Act (17 USC §108) does not require AMS’s permission. Republication, systematic reproduction, posting in electronic form, such as on a website or in a searchable database, or other uses of this material, except as exempted by the above statement, requires written permission or a license from AMS. All AMS journals and monograph publications are registered with the Copyright Clearance Center (<https://www.copyright.com>). Additional details are provided in the AMS Copyright Policy statement, available on the AMS website (<https://www.ametsoc.org/PUBSCopyrightPolicy>).

Supplementary Material for “**Recent trends in summer atmospheric circulation in the North Atlantic/European region: is there a role for anthropogenic aerosols?**”

Buwen Dong and Rowan T. Sutton

National Centre for Atmospheric Science, Department of Meteorology,
University of Reading, Reading, UK.

Correspondence author address: Buwen Dong, Department of Meteorology, University of Reading, Reading, RG6 6BB. UK. E-mail: b.dong@reading.ac.uk

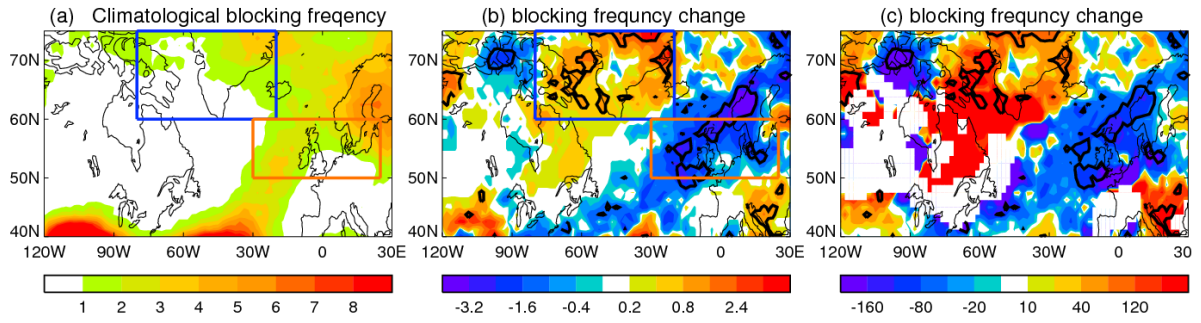


Figure S1. (a) Climatological blocking frequency (%) in JJA based on NCEP reanalysis. (b, c) changes and percentage changes of blocking frequency between two periods. Thick lines in (b, c) highlight regions where differences are statistically significant at 10% level based on the two tailed Student's t-test.

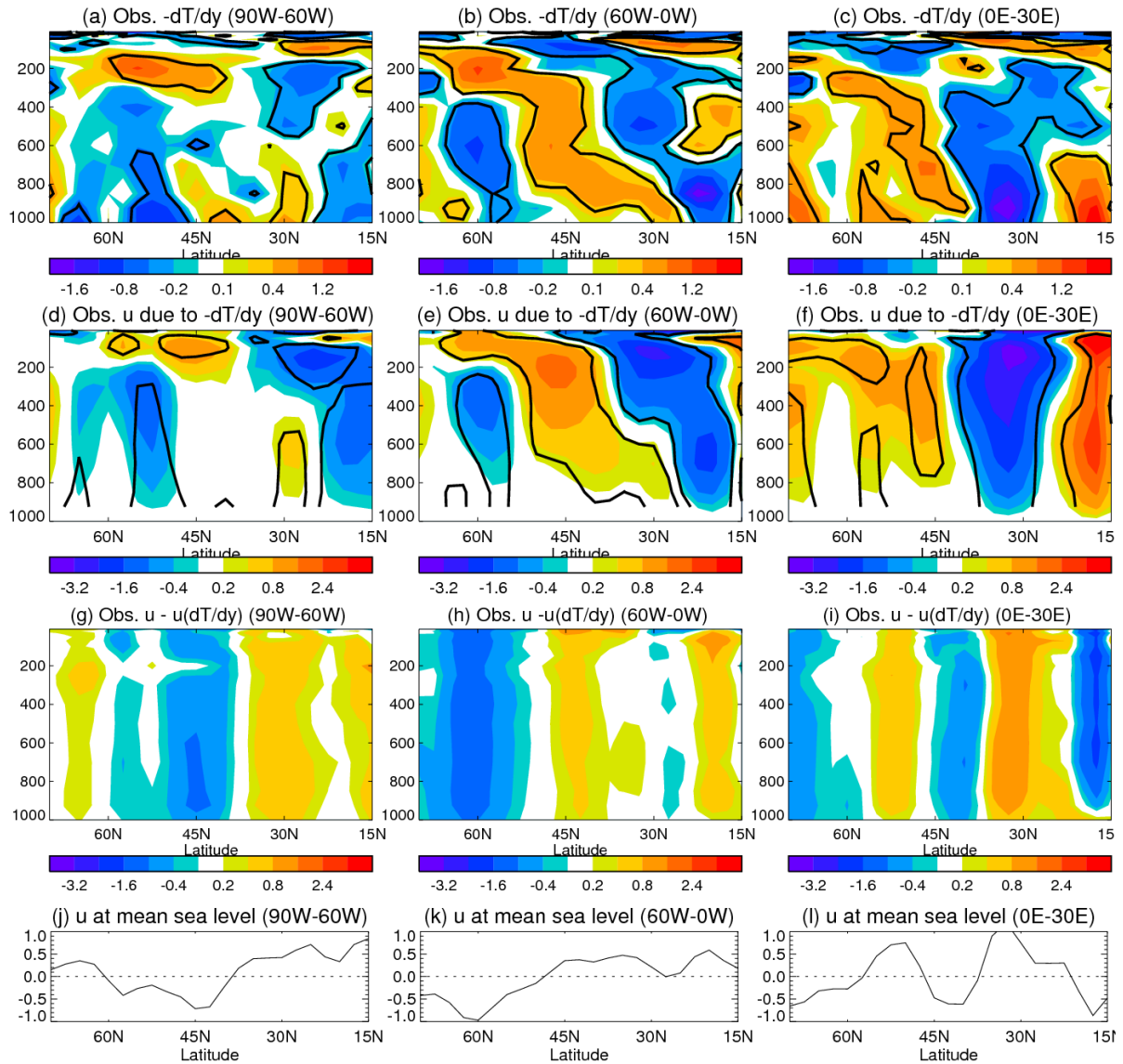


Figure S2. Decadal changes at three sectors of ($90^{\circ}\text{W}-60^{\circ}\text{W}$), ($60^{\circ}\text{W}-0$), and ($0^{\circ}-30^{\circ}\text{E}$) between 1994-2011 and 1964-1981 in JJA based on the NCEP reanalysis. (a, b, c) meridional temperature gradient ($^{\circ}\text{K}$ per 1000 km), (d, e, f) zonal wind changes from the thermal wind balance related to meridional temperature gradient, (g, h, i) zonal wind change residual, and (j, k, l) geostrophic zonal wind changes at mean sea level from SLP changes. Thick lines highlight regions where differences are statistically significant at 10% level based on the two-tailed Student's t-test.

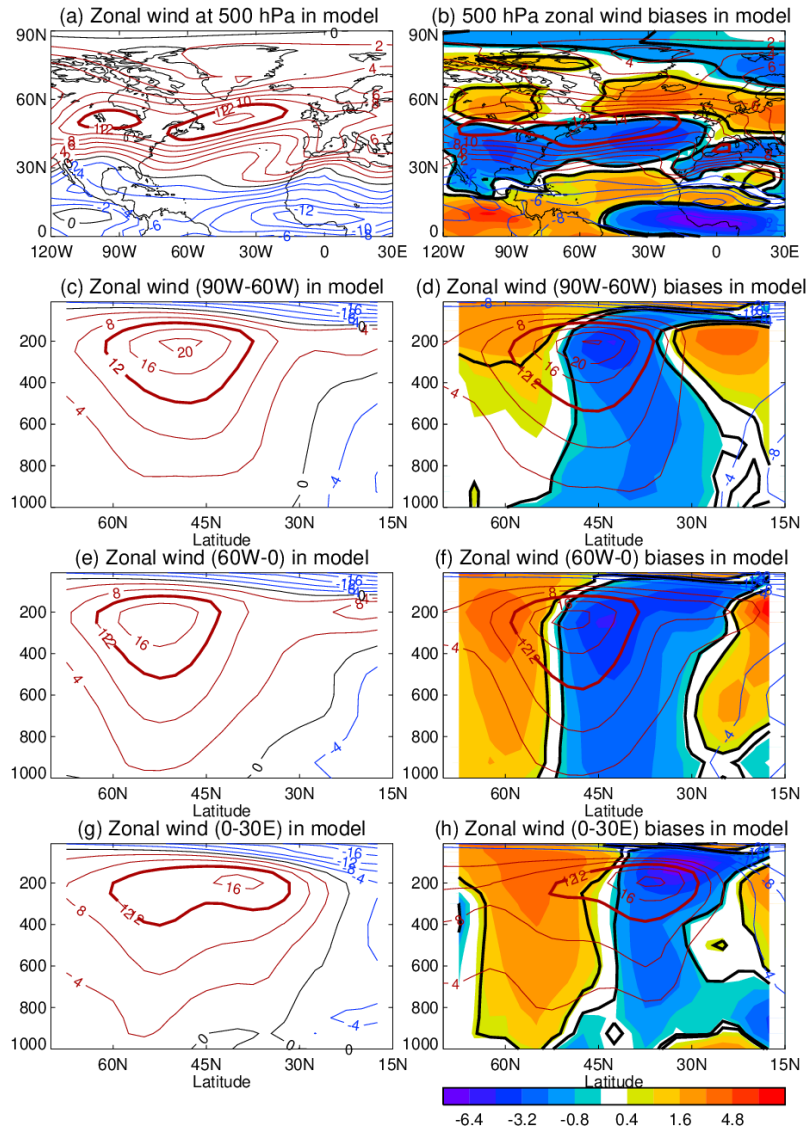


Figure S3. Model simulated climatological zonal wind (m s^{-1}) over the period 1994-2011 at 500 hPa (a) and at three zonal sectors of ($90^{\circ}\text{W}-60^{\circ}\text{W}$), ($60^{\circ}\text{W}-0^{\circ}$), and ($0^{\circ}-30^{\circ}\text{E}$) (c, e, g) in JJA. (b, d, f, h) zonal wind biases (colour) (ALL – reanalysis) with zonal wind based on the NCEP reanalysis in contours. Thick lines (right column) highlight regions where differences are statistically significant at 10% level based on the two tailed Student’s t-test. Note the colour scales for biases are doubled in comparison with those in observed changes shown in Figure 2.

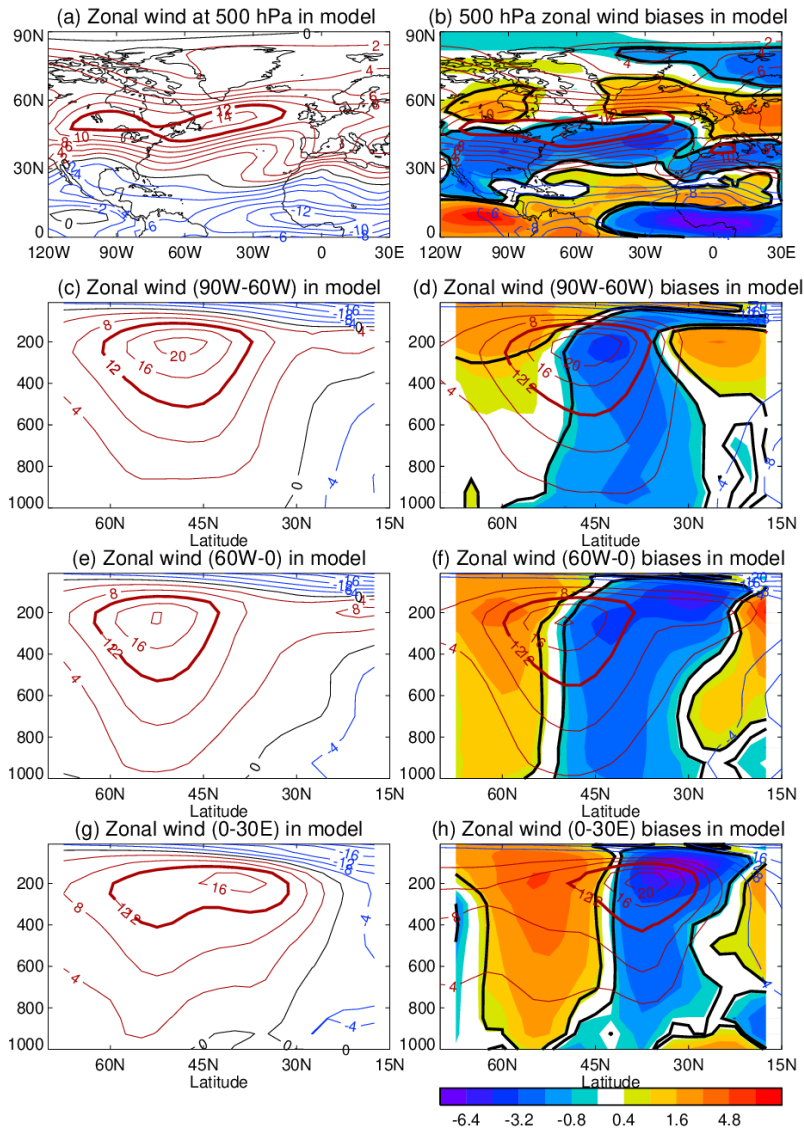


Figure S4. Model simulated climatological zonal wind (m s^{-1}) combined over the two periods of 1964-1981 and 1994-2011 at 500 hPa (a) and at three zonal sectors of ($90^{\circ}\text{W}-60^{\circ}\text{W}$), ($60^{\circ}\text{W}-0^{\circ}$), and ($0^{\circ}-30^{\circ}\text{E}$) (c, e, g) in JJA. (b, d, f, h) zonal wind biases (colour) (mean of ALL and CON – mean of reanalysis of two periods) with zonal wind based on the NCEP reanalysis in contours. Thick lines (right column) highlight regions where differences are statistically significant at 10% level based on the two tailed Student's t-test. Note the colour scales for biases are doubled in comparison with those in observed changes shown in Figure 2.

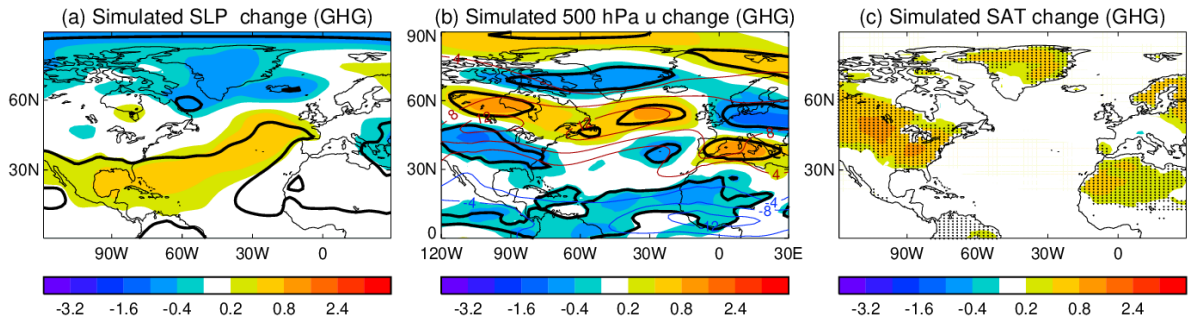


Figure S5. Simulated climatological seasonal mean (JJA) responses of (a) SLP (hPa), (b) zonal wind (m s^{-1}) at 500 hPa, and (c) surface air temperature ($^{\circ}\text{C}$) to changes in GHGs (ALL-SSTAA). Thin red (westerly) and blue (easterly) lines in (b) are the climatology of the CON simulation. Thick lines (a, b) and dots (c) highlight regions where differences are statistically significant at 10% level based on the two tailed Student's t-test.

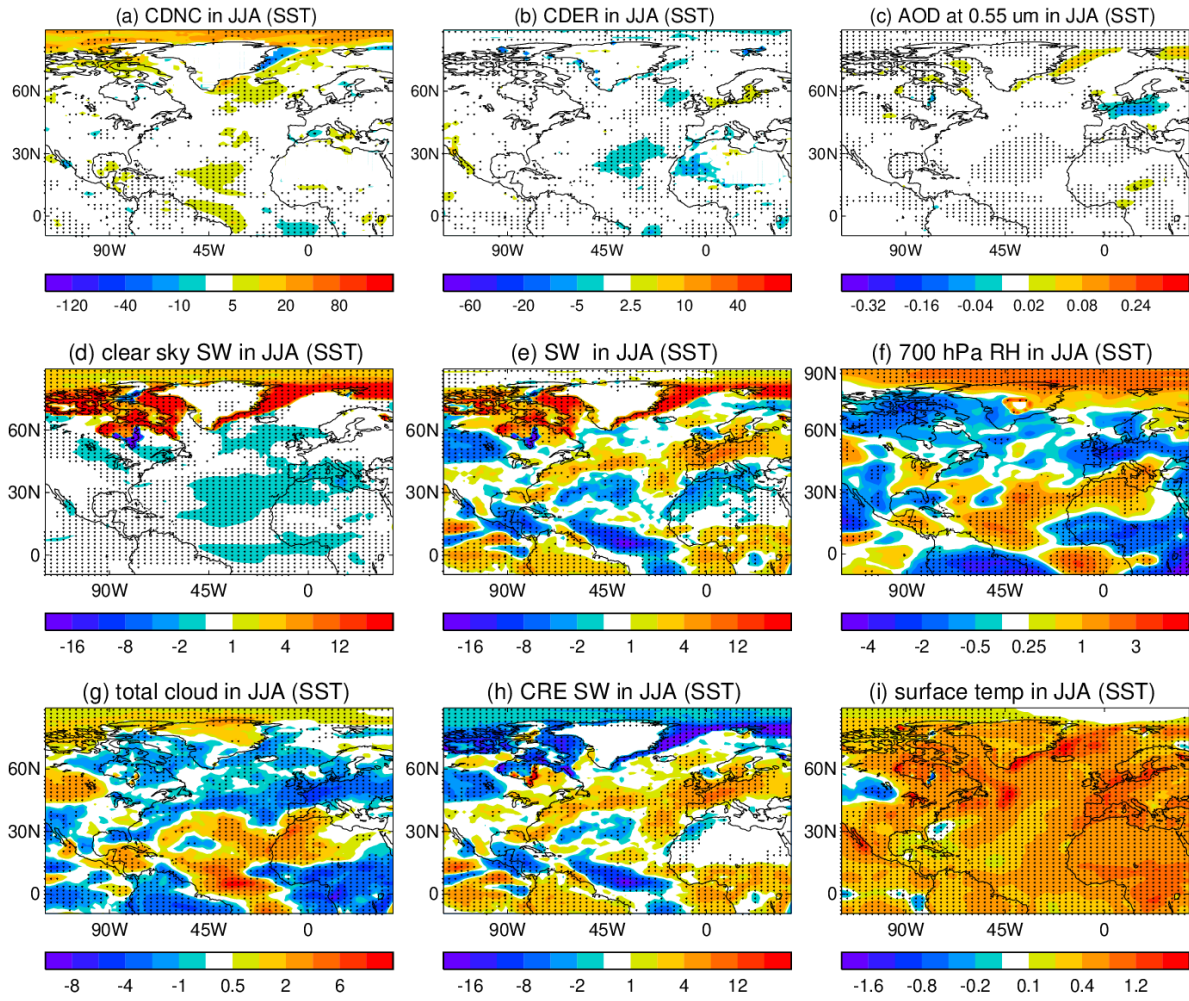


Figure S6. Simulated climatological seasonal mean responses in JJA in response to changes in SST/SIE (SST- CON). (a) cloud droplet number concentration (CDNC), (b) cloud droplet effective radius (CDER), (c) AOD at 0.55 μm , (d) surface clear sky SW radiation, (e) surface SW radiation, (f) relative humidity at 700 hPa (%), (g) cloud fraction (%), (h) surface shortwave cloud radiative effect (CRE SW), (i) surface temperature ($^{\circ}\text{C}$). Radiations are positive downwards. Changes in CDCN and CDER are percentage changes relative to the experiment CON. Dots or thick lines highlight regions where differences are statistically significant at 10% level based on the two tailed Student's t-test.

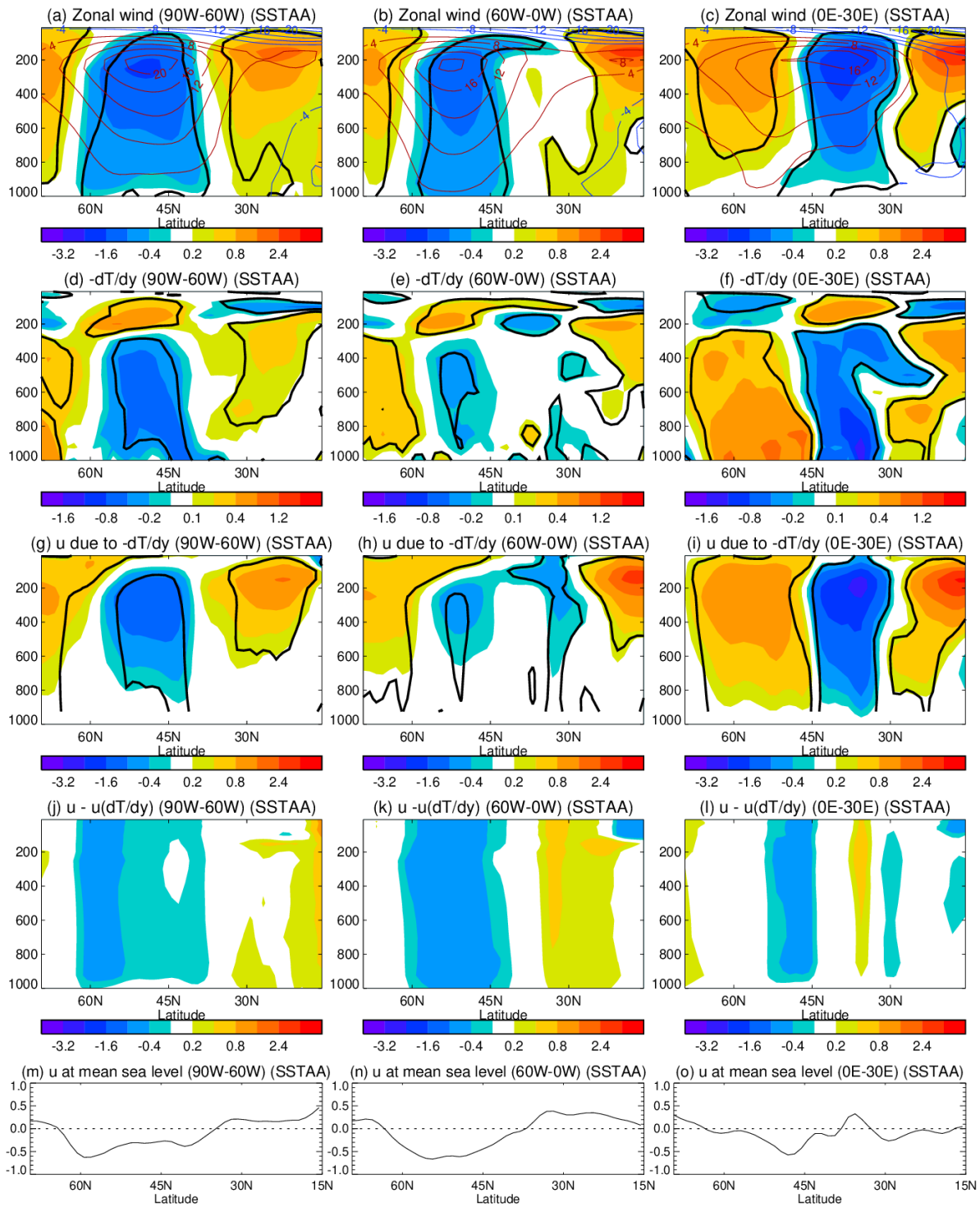


Figure S7. Simulated (a, b, c) zonal wind changes (m s^{-1}), (d, e, f) meridional temperature gradient ($^{\circ}\text{K}$ per 1000 km), (g, h, i) zonal wind changes from the thermal wind balance related to meridional temperature gradient, (j, k, l) zonal wind change residual, and (m, n, o) geostrophic zonal wind changes at mean sea level from SLP changes at three sectors of (90°W - 60°W), (60°W - 0°), and (0° - 30°E) in response to combined changes in AA and SST/SIE (SSTAA-CON). Thin red (westerly) and blue (easterly) lines (a, b, c) are the climatology of the CON simulation. Thick lines highlight regions where differences are statistically significant at 10% level based on the two tailed Student's t-test.